PERGAMON

Engineering Fracture Mechanics 61 (1998) 655–671

Engineering Fracture Mechanics

BEM based evaluation of SIFs using modified crack closure integral technique under remote and/or crack edge loading

N.K. Mukhopadhyay[a], S.K. Maiti[b], A. Kakodkar[a]

[a]*Reactor Design & Development Group, Bhabha Atomic Research Centre, Mumbai 400085, India*
[b]*Mechanical Engineering Department, Indian Institute of Technology, Bombay, Mumbai 400076, India*

Received 20 September 1997; received in revised form 1 June 1998

Abstract

This paper deals with the boundary element method based evaluation of stress intensity factors for mode I and mixed mode problems under remote and/or crack edge loading. The modified crack closure integral technique has been used to enhance the accuracy of the computed stress intensity factors. Simple, ready to use, relations for the strain energy release rate have been obtained corresponding to linear, quadratic and quarter point elements surrounding the crack tip. The boundary element method is employed by breaking a domain into two subregions for the mixed mode problems. Case studies involving remote or crack edge loading for both mode I and mixed mode problems are presented to demonstrate the accuracy of the new scheme. The stress intensity factors based on the proposed scheme show better agreement with the standard solutions available in the literature than those obtained directly through the displacement method.

Keywords: BEM; Modified crack closure integral; SIFs; Remote loading; Crack edge loading; Mixed mode; Subregion analysis

Nomenclature

a	crack length
c_n	coefficients of traction in MCCI formulation
E	elastic modulus
G_{I}, G_{II}	strain energy release rate in mode I, mode II
K_{I}, K_{II}	stress intensity factors
l	crack tip element length
L, L_1, L_2,W	domain geometric dimensions

0013-7944/98/$ - see front matter
PII: S0013-7944(98)00040-X

p, q	components of crack edge loading normal and parallel to crack
r_1, r_2	internal and external radii
s_j, S	components of traction parallel to crack and global x direction
t_j, T	components of traction normal to crack and global y direction
u, U	components of displacement parallel to crack and global x direction
v, V	components of displacement normal to crack and global y direction
W_{I}, W_{II}	crack closure work
x, y	cartesian coordinates
Y	SIF correction factor
θ	crack orientation with x-axis
μ	shear modulus
ν	Poisson's ratio
ξ	natural coordinate

1. Introduction

The boundary element method (BEM) is a well established numerical tool for computation of stress intensity factors (SIFs) with good accuracy [1–16]. In the case of modelling of mixed mode problems by the BEM a close proximity of nodes on the two crack edges leads to a degeneracy of the boundary element equations [2]. This shortcoming is overcome using the subregion analysis, which was first introduced by Blandford et al. [6] to solve problems of mixed mode cracks. In this scheme, the nodes which are on the two crack edges are assumed to lie on two adjacent regions. The two regions have a common interface. The boundary element equations are written for each region separately [6]. The equations connected with the common interface nodes are obtained from the two subregions. Two conditions are invoked to combine the sets of equations associated with the subregions to obtain a sufficient number of equations for the whole domain. First, any node common to the two adjacent subregions must have the same displacements. Second, net traction at the nodes must be zero. As has been pointed out by Cruse [1] the real shortcoming of this method is the need to create non-physical surfaces extending from the original crack tip to the physical boundaries. However this method is simple, easy to implement and poses no serious difficulty except for studying the path of the crack growth phenomena. A large number of investigators followed this technique to analyse mixed mode crack problems [8–10, 13]. The single domain BEM [17–19] using hypersingular boundary integral equations do not require any subdivisioning of the geometry. In the single domain BEM, the displacement equation is applied one crack edge/surface and traction equation on the other crack edge/surface. In the present paper the multi-domain formulation is adapted.

The crack closure integral concept has been adapted in the finite element method (FEM) [20–24] to estimate the SIF. Farris and Liu [15] reported the SIFs based on the crack closure integrals and the BEM for three dimensional components. Their results show good agreement with the standard solutions. The present authors have demonstrated recently [25, 26] that the

MCCI technique can be adapted in the BEM to enhance the computational accuracy of the SIFs. The case studies reported so far deal with the mode I problems only.

Loading on the crack edges come up due to explicit mechanical loading, crack subjected to fluid pressure, implicit loading arising out of a thermal field, etc. In such a case, when a crack is extended or an extended crack is closed, to compute the crack closure work, there is an extra loading on the newly formed crack edges on top of the usual crack closure forces. This loading contributes to an additional amount of work. A crack closure integral calculation must therefore cognise this fact. Such calculations have been presented earlier in the case of FEM [24]. This is not yet reported in the case of BEM.

In this paper, the effectiveness of the MCCI in conjunction with the local smoothing scheme is demonstrated for the mixed mode problems. Further, the evaluations of crack closure integrals in the presence of crack edge loading are presented.

2. Mathematical formulation

In the case of mechanical loading applied away from the crack edges (Fig.1a), the nodes $j-2$ and $j-1$ on the crack edge AO are free of any load. As the crack extends up to B, the newly formed crack edges are also load-free (Fig. 1b). If the crack edges are subjected to, say, fluid pressure (Fig. 1c), as the crack extends, the newly formed crack edges are also subjected to the same fluid pressure (Fig. 1d). The crack edges will therefore undergo an extra opening. The crack closure work have two parts. One part is due to the usual tractions t_j , t_{j+1} and t_{j+2} and the other part is due to fluid pressure p. For a mode I problem the crack closure work is given by

$$W_{\mathrm{I}} = \frac{1}{2}\int_0^l v\,t\,\mathrm{d}x + \frac{1}{2}\int_0^l v\,p\,\mathrm{d}x \tag{1}$$

where p is intensity of distributed crack edge normal load and v is full opening displacement. In the absence of fluid pressure W_{I} is fully given by the first part.

Similarly for a mode II crack the crack closure work

$$W_{\mathrm{II}} = \frac{1}{2}\int_0^l u\,s\,\mathrm{d}x + \frac{1}{2}\int_0^l u\,q\,\mathrm{d}x \tag{2}$$

where u is the full crack sliding displacement, s is the traction and q is intensity of distributed external shear load on the crack edges. The direction of this load is positive, when it produces effects additive to that due to the external load. The shown directions are positive. The integrals can be computed following a procedure given in Ref. [26]. The pressure loading can be of uniform intensity or with a linear or quadratic variation. In the following, results are given for crack edges subjected to constant "fluid" pressure. The results for any variation can be obtained easily following the procedure given below.

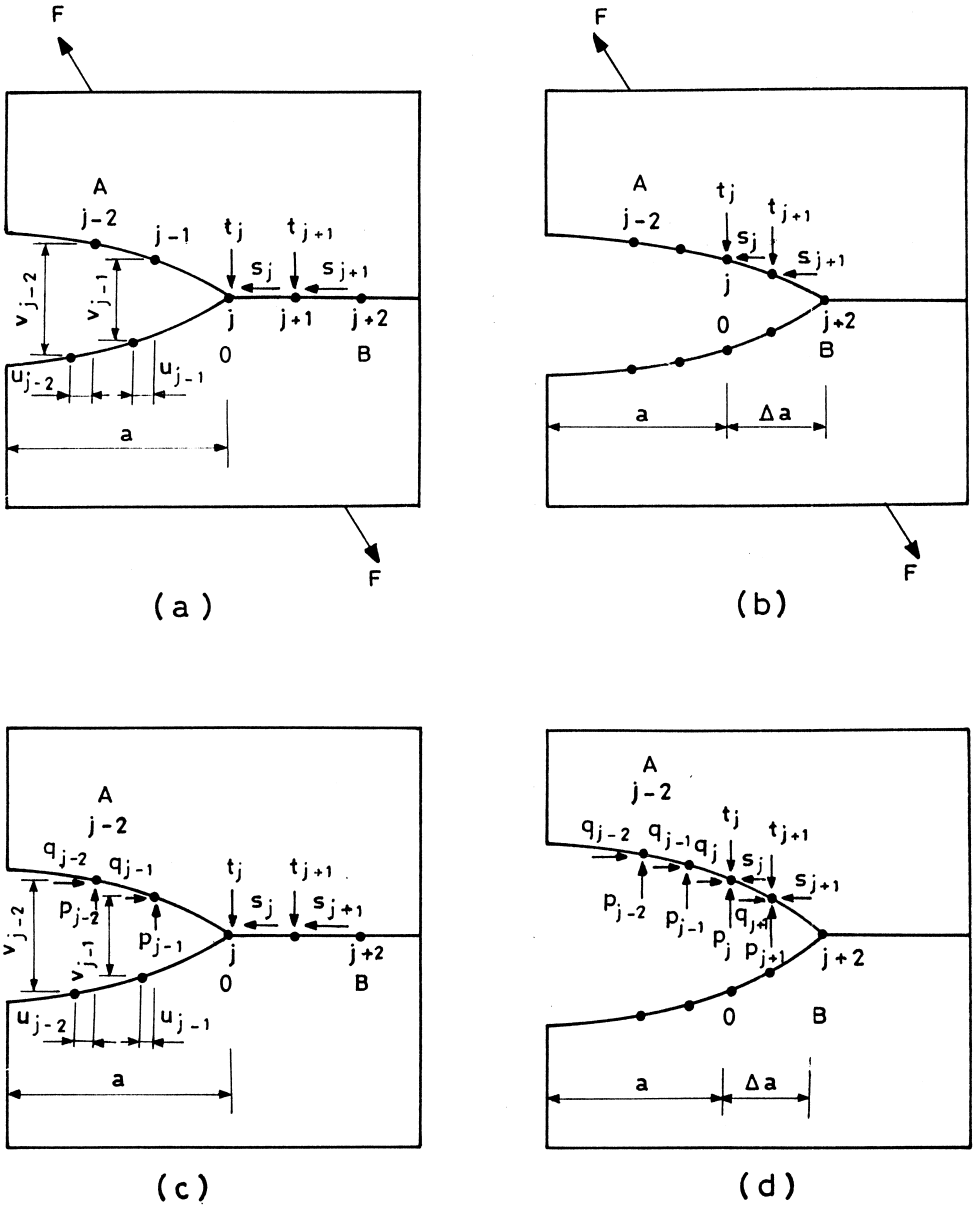

Fig. 1. Illustration of crack closure forces. (a) Remote loading and (b) closure forces, (c) crack edge loaded externally and (d) closure forces and external loading.

Under a mixed mode loading, the upper and lower crack faces do not deform symmetrically or antisymmetrically with respect to the crack plane. The amount of work involved in the symmetric and antisymmetric deformations can be easily obtained through a judicious partitioning of the domain.

2.1. Linear element

The displacement variation over OA for linear element can be written in the form

$$v = v_{j-1}(1-\xi)/2 \tag{3}$$

where ξ is a natural coordinate with origin at the centre of OA and v_{j-1} is the opening displacement at corner node A. A linear variation of the traction t along OB can be represented in the same way.

$$t = 0.5\,(t_j + t_{j+1}) - 0.5\,(t_j - t_{j+1})\xi \tag{4}$$

where ξ is a natural coordinate with origin at the centre of OB. The crack edges are subjected to constant fluid pressure p. The crack closure work is obtained from Eq. (1).This gives the energy release rate

$$G_{\mathrm{I}} = v_{j-1}\,(c_1\,t_j + c_2\,t_{j+1} + c_3\,p)/12 \tag{5}$$

where $c_1 = 2$, $c_2 = 1$ and $c_3 = 3$.

A similar expression can be derived for G_{II} for a mode II case, involving x components of tractions and displacements.

$$G_{\mathrm{II}} = u_{j-1}\,(c_1\,s_j + c_2\,s_{j+1} + c_3\,q)/12. \tag{6}$$

The SIF can then be obtained using the standard relations between G and K.

2.2. Quadratic element

In the case of quadratic elements (Fig. 1a) the displacement variation over OA is given by

$$v = v_{j-1} - 0.5\,v_{j-2}\,\xi + (0.5\,v_{j-2} - v_{j-1})\,\xi^2. \tag{7}$$

Similarly the traction variation, which is also quadratic, has the form

$$t = t_{j+1} + 0.5\,(t_{j+2} - t_j)\,\xi + \left[0.5\,(t_{j+2} + t_j) - t_{j+1}\right]\xi^2. \tag{8}$$

The total crack closure work in the opening mode

$$\begin{aligned} W_{\mathrm{I}} &= \frac{1}{2}\int_0^l v\,t\,\mathrm{d}x + \frac{1}{2}\int_0^l v\,p\,\mathrm{d}x \\ &= \left[v_{j-1}(2\,t_j + 16\,t_{j+1} + 2\,t_{j+2}) + v_{j-2}(4\,t_j + 2\,t_{j+1} - t_{j+2})\right]/60 + p(4\,v_{j-1} + v_{j-2})/12. \end{aligned} \tag{9}$$

The strain energy release rates

$$G_{\mathrm{I}} = \left[v_{j-1}\,(c_1\,t_j + c_2\,t_{j+1} + c_3\,t_{j+2} + c_4\,p) + v_{j-2}\,(c_5\,t_j + c_6\,t_{j+1} + c_7\,t_{j+2} + c_8\,p)\right]/60 \tag{10}$$

$$G_{II} = \left[u_{j-1}\,(c_1\,s_j + c_2\,s_{j+1} + c_3\,s_{j+2} + c_4\,q) + u_{j-2}\,(c_5\,s_j + c_6\,s_{j+1} + c_7\,s_{j+2} + c_8\,q)\right]/60 \tag{11}$$

where $c_1 = 2$, $c_2 = 16$, $c_3 = 2$, $c_4 = 20$, $c_5 = 4$, $c_6 = 2$, $c_7 = -1$ and $c_8 = 5$.

2.3. Quarter point element

In the case of quarter point elements the displacement is assumed to vary as $\sqrt{x}$ along OA. That is

$$v = 2\,(v_{j-2} - 2\,v_{j-1})\,(1 - x/l) + (4\,v_{j-1} - v_{j-2})\sqrt{(1 - x/l)}. \tag{12}$$

The traction too has a similar variation and can be represented in the form

$$t = t_j\left\{-0.5\,\xi\,(1-\xi)\right\} + t_{j+1}\,(1-\xi^2) + t_{j+2}\left\{0.5\,\xi\,(1+\xi)\right\} \tag{13}$$

where $1 + \xi = 2\sqrt{(x/l)}$.

The total crack closure work in the opening mode

$$\begin{aligned} W_I &= \frac{1}{2}\int_0^l v\,t\,\mathrm{d}x + \frac{1}{2}\int_0^l v\,p\,\mathrm{d}x \\ &= \Big[v_{j-1}\left\{t_j\,(140 - 45\pi) + t_{j+1}\,(60\pi - 176) + t_{j+2}\,(56 - 15\pi)\right\} \\ &\quad + v_{j-2}\left\{t_j\,(11.25\pi - 34) + t_{j+1}\,(56 - 15\pi) + t_{j+2}\,(3.75\pi - 12)\right\}\Big]/60 \\ &\quad + p\left\{2\,v_{j-1} + v_{j-2}\right\}/6. \end{aligned} \tag{14}$$

The strain energy release rates in mode I and mode II are finally obtained as

$$G_I = \left[v_{j-1}(c_1\,t_j + c_2\,t_{j+1} + c_3\,t_{j+2} + c_4\,p) + v_{j-2}(c_5\,t_j + c_6\,t_{j+1} + c_7\,t_{j+2} + c_8\,p)\right]/60 \tag{15}$$

$$G_{II} = \left[u_{j-1}(c_1\,s_j + c_2\,s_{j+1} + c_3\,s_{j+2} + c_4\,q) + u_{j-2}(c_5\,s_j + c_6\,s_{j+1} + c_7\,s_{j+2} + c_8\,q)\right]/60 \tag{16}$$

where

$$\begin{aligned} &c_1 = (140 - 45\pi),\ c_2 = (60\pi - 176),\ c_3 = (56 - 15\pi),\ c_4 = 20, \\ &c_5 = (11.25\pi - 34),\ c_6 = (56 - 15\pi),\ c_7 = (3.75\pi - 12) \text{ and } c_8 = 10. \end{aligned}$$

3. Case studies

Five case studies involving an angled edge crack, angled crack, a centre crack under fluid pressure, a radial inner edge crack under internal pressure in a cylindrical vessel and a kinked crack, are presented. The results are all based on plane strain condition. All the cases have been studied considering the material to be isotropic and using linear, quadratic and quarter point elements. The computed SIFs, wherever possible, are compared with the standard solutions available in the literature. All computations are based on single precision arithmetic on a PC 486.

3.1. Angled edge crack

The crack is under remote loading (Fig. 2). The major dimensions are: $H_1 = H_2 = W = 20$ mm and $a/W = 0.5$. The material properties are: shear modulus $\mu = 10^5$ MPa and Poisson's ratio $\nu = 0.3$. The crack angle θ is varied from 15° to 60°. The analysis is based on the subregion technique. The whole plate is divided into two subregions. Each subregion is modelled using 25 elements when quadratic and quarter point elements are employed. The crack edge is modelled by six elements. The first few elements ahead of the crack tip, forming a part of the interface are oriented at an angle θ (Fig. 2b), where θ is the crack orientation. The remaining interface is oriented horizontally. This arrangement helps in an evaluation of the MCCI for an in-plane extension of the crack. The crack tip element size is $0.02a$ and the sizes of the subsequent elements, away from the crack tip are $0.04a$, $0.08a$, $0.16a$, etc. The same nodal arrangements have been employed for the case of linear elements. Here the total number of elements is 50 and the crack tip element size is $0.01a$. The sizes of subsequent elements away from the crack tip vary accordingly.

From the standard BE analysis, the global displacements and tractions are obtained. These are resolved into components (s, t and u, v) aligned with the normal and parallel directions of the crack edges. That is, $s = S\cos\theta + T\sin\theta$, $t = S\sin\theta - T\cos\theta$, $u = U\cos\theta + V\sin\theta$, $v = U\sin\theta - V\cos\theta$, where S and T are tractions and U and V are displacements in global x and y directions, respectively. These tractions and displacements can be used to compute G_{I} and G_{II} using the relations given earlier.

In the following, the SIFs has been computed using both the displacement method and the proposed MCCI method. In the displacement method the SIF is evaluated considering separately the displacement of the first and the second corner nodes behind the crack tip. The

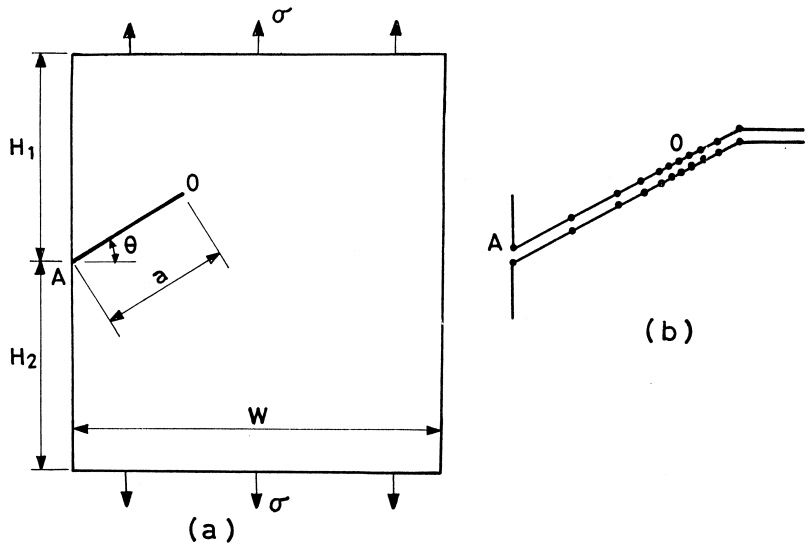

Fig. 2. (a) Angled edge crack and (b) boundary element mesh over span of crack.

results in the form of SIF correction factor Y ($Y = K_I/\sigma\sqrt{(\pi a)}$ or $Y = K_{II}/\sigma\sqrt{(\pi a)}$) are compared with some standard solutions [27, 28] in Table 1.

Table 1
Comparison of SIF correction factor Y for mixed mode angled edge crack ($a/W = 0.5$) for linear, quadratic and quarter point elements

	SIF correction factor Y							
			Computed by:					
			Displacement method				CCI method	
			2nd corner node		1st corner node			
θ, mode	Reference solution [28]	Ref. [27]	Y	% Error	Y	% Error	Y	% Error
Linear element								
15.0, I		2.5476	2.4120		2.2858		2.4346	
15.0, II		0.3696	0.3369		0.3215		0.3442	
22.5, I	2.2800	2.2547	2.1501	−5.699	2.0375	−10.634	2.1701	−4.822
22.5, II	0.4950	0.5003	0.4565	−7.771	0.4356	−11.993	0.4664	−5.782
30.0, I		1.9056	1.8353		1.7391		1.8521	
30.0, II		0.5788	0.5276		0.5033		0.5389	
45.0, I	1.2000	1.2305	1.1896	−0.870	1.1267	−6.112	1.1994	−0.052
45.0, II	0.5700	0.5850	0.5373	−5.737	0.5125	−10.089	0.5486	−3.758
60.0, I			0.6439		0.6087		0.6470	
60.0, II			0.4312		0.4112		0.4401	
Quadratic element								
15.0, I		2.5476	2.5543		2.4631		2.5875	
15.0, II		0.3696	0.3473		0.3445		0.3666	
22.5, I	2.2800	2.2547	2.2701	−0.435	2.1888	−4.001	2.2992	0.843
22.5, II	0.4950	0.5003	0.4681	−5.430	0.4642	−6.217	0.4940	−0.211
30.0, I		1.9056	1.9346		1.8645		1.9582	
30.0, II		0.5788	0.5392		0.5344		0.5685	
45.0, I	1.2000	1.2305	1.2556	4.636	1.2073	0.609	1.2411	3.425
45.0, II	0.5700	0.5850	0.5457	−4.259	0.5405	−5.172	0.5749	0.855
60.0, I			0.6904		0.6580		0.6877	
60.0, II			0.4322		0.4282		0.4555	
Quarter point element								
15.0, I		2.5476	2.6027		2.5599		2.5213	
15.0, II		0.3696	0.3532		0.3573		0.3566	
22.5, I	2.2800	2.2547	2.3126	1.429	2.2742	−0.253	2.2398	−1.763
22.5, II	0.4950	0.5003	0.4759	−3.850	0.4814	−2.757	0.4803	−2.966
30.0, I		1.9056	1.9703		1.9368		1.9071	
30.0, II		0.5788	0.5480		0.5538		0.5526	
45.0, I	1.2000	1.2305	1.2784	6.536	1.2538	4.485	1.2335	2.792
45.0, II	0.5700	0.5850	0.5543	−2.751	0.5599	−1.769	0.5586	−2.007
60.0, I			0.7030		0.6835		0.6696	
60.0, II			0.4389		0.4434		0.4423	

3.2. Angled crack

The subregion technique is again employed to study the angled crack in a finite plate under uniform tension (Fig. 3). The configuration of the plate is: $W = 50$ mm, $H = 100$ mm. The crack angle θ is varied from 15° to 75° in steps of 15°. The a/W ratio is 0.2. The material properties mentioned in the earlier case have again been used. The whole plate is divided into two subregions (Fig. 3b). The discretization details are again the same as in the previous case. The computed SIF correction factor Y ($Y = K_I/\sigma\sqrt{(\pi a)}$ or $Y = K_{II}/\sigma\sqrt{(\pi a)}$) based on the displacement and MCCI techniques have been compared in Table 2.

The same example is studied by varying the a/W ratio. The computed SIF correction factor Y using only the MCCI technique is compared with the standard solutions for two a/W ratios, 0.4 and 0.6, in Table 3.

3.3. Centre crack under fluid pressure

The geometry ($L = W = 10$ mm; $a/W = 0.1$) and loading is shown in Fig. 4. Material data are: elastic modulus $E = 2.1\times10^5$ MPa and $\nu = 0.3$. One fourth of the plate is discretized. The SIF is computed using displacements at the first and second corner nodes and the MCCI method. In the latter case, the SIF is evaluated with and without the inclusion of the crack edge external loads. The SIF correction factor, $Y = K_I/p\sqrt{(\pi a)}$ is compared in Table 4.

3.4. Radial crack under fluid pressure

For this case, parameter $a/(r_2 - r_1)$ is varied in the range of 0.2–0.8 (Fig. 5). The number of elements are 26 and 52, respectively, when quadratic and quarter point elements are used. The

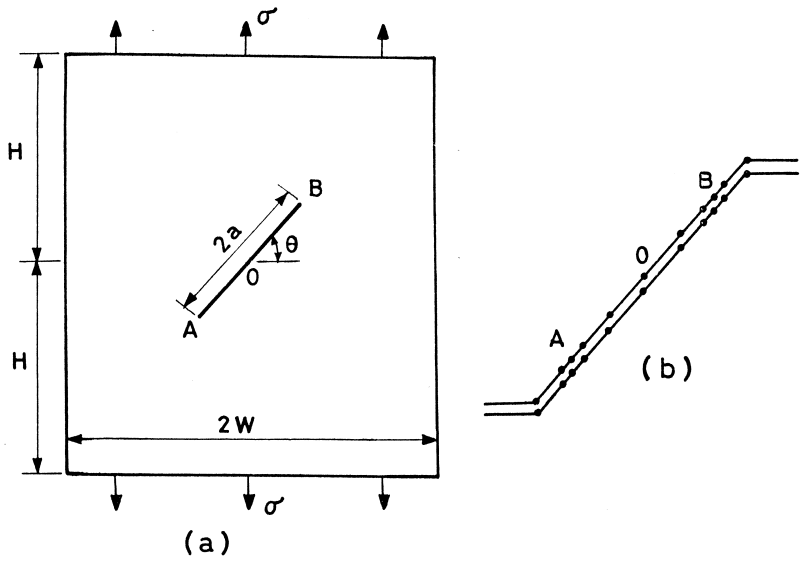

Fig. 3. (a) Angled crack and (b) boundary element mesh over span of crack.

Table 2
Comparison of SIF correction factor Y for angled crack ($a/W = 0.2$) for linear, quadratic and quarter point elements

	SIF correction factor Y						
		Computed by:					
		Displacement method				CCI method	
		2nd corner node		1st corner node			
θ, mode	Reference solution [29]	Y	% Error	Y	% Error	Y	% Error
Linear element							
15.0, I	0.9577	0.8973	−6.306	0.8571	−10.505	0.9185	−4.093
15.0, II	0.2510	0.2357	−6.095	0.2252	−10.280	0.2413	−3.879
30.0, I	0.7730	0.7244	−6.286	0.6920	−10.481	0.7416	−4.061
30.0, II	0.4367	0.4092	−6.297	0.3909	−10.486	0.4189	−4.078
45.0, I	0.5181	0.4862	−6.160	0.4645	−10.346	0.4978	−3.909
45.0, II	0.5072	0.4738	−6.585	0.4525	−10.785	0.4848	−4.423
60.0, I	0.2605	0.2459	−5.591	0.2351	−9.756	0.2521	−3.212
60.0, II	0.4417	0.4113	−6.889	0.3927	−11.098	0.4206	−4.777
75.0, I	0.0701	0.0683	−2.567	0.0654	−6.679	0.0703	0.255
75.0, II	0.2560	0.2395	−6.430	0.2289	−10.587	0.2453	−4.161
Quadratic element							
15.0, I	0.9577	0.9111	−4.866	0.9080	−5.190	0.9680	1.079
15.0, II	0.2510	0.2389	−4.823	0.2382	−5.110	0.2540	1.215
30.0, I	0.7730	0.7357	−4.828	0.7332	−5.145	0.7818	1.133
30.0, II	0.4367	0.4156	−4.831	0.4143	−5.123	0.4418	1.177
45.0, I	0.5181	0.4936	−4.721	0.4921	−5.015	0.5248	1.300
45.0, II	0.5072	0.4828	−4.818	0.4812	−5.136	0.5130	1.145
60.0, I	0.2605	0.2488	−4.485	0.2482	−4.704	0.2650	1.716
60.0, II	0.4417	0.4209	−4.720	0.4194	−5.038	0.4473	1.257
75.0, I	0.0701	0.0677	−3.397	0.0676	−3.502	0.0724	3.246
75.0, II	0.2560	0.2457	−4.026	0.2455	−4.114	0.2624	2.505
Quarter point element							
15.0, I	0.9577	0.9252	−3.396	0.9401	−1.833	0.9398	−1.867
15.0, II	0.2510	0.2425	−3.382	0.2465	−1.794	0.2466	−1.742
30.0, I	0.7730	0.7471	−3.351	0.7593	−1.778	0.7592	−1.785
30.0, II	0.4367	0.4219	−3.395	0.4288	−1.813	0.4290	−1.771
45.0, I	0.5181	0.5013	−3.245	0.5095	−1.652	0.5097	−1.618
45.0, II	0.5072	0.4900	−3.383	0.4979	−1.826	0.4980	−1.811
60.0, I	0.2605	0.2527	−3.006	0.2570	−1.342	0.2574	−1.173
60.0, II	0.4417	0.4271	−3.299	0.4340	−1.747	0.4341	−1.716
75.0, I	0.0701	0.0688	−1.835	0.0701	0.048	0.0705	0.523
75.0, II	0.2560	0.2493	−2.601	0.2540	−0.780	0.2548	−0.474

sizes of elements near the crack tip are $0.01a$, $0.02a$, $0.04a$, $0.08a$ etc. For the linear element the same discretization has been employed and the number of elements and nodes is 52. The SIFs are computed using the proposed scheme with and without the inclusion of fluid pressure. A comparison of SIF correction factor Y ($Y = K_I/p\sqrt{(\pi a)}$) is presented in Table 5.

Table 3
Comparison of SIF correction factor Y for angled crack

	SIF correction factor Y						
		Computed by CCI method					
		Linear element		Quadratic element		Quarter point element	
θ, mode	Reference solution [29]	Y	% Error	Y	% Error	Y	% Error
$a/w = 0.4$							
15.0, I	1.0402	0.9949	−4.354	1.0504	0.977	1.0210	−1.850
15.0, II	0.2560	0.2456	−4.065	0.2587	1.070	0.2514	−1.814
30.0, I	0.8456	0.8078	−4.471	0.8538	0.967	0.8300	−1.849
30.0, II	0.4497	0.4306	−4.244	0.4546	1.092	0.4417	−1.787
45.0, I	0.5719	0.5457	−4.589	0.5775	0.976	0.5613	−1.847
45.0, II	0.5290	0.5046	−4.604	0.5344	1.027	0.5191	−1.868
60.0, I	0.2896	0.2771	−4.319	0.2932	1.234	0.2851	−1.553
60.0, II	0.4660	0.4426	−5.030	0.4708	1.027	0.4574	−1.853
75.0, I	0.0783	0.0766	−2.214	0.0800	2.170	0.0779	−0.463
75.0, II	0.2721	0.2577	−5.291	0.2758	1.344	0.2679	−1.533
$a/w = 0.6$							
15.0, I	1.2183	1.1529	−5.371	1.2209	0.215	1.1884	−2.451
15.0, II	0.2725	0.2603	−4.487	0.2742	0.609	0.2664	−2.227
30.0, I	0.9840	0.9286	−5.633	0.9860	0.198	0.9597	−2.465
30.0, II	0.4800	0.4566	−4.877	0.4827	0.554	0.4691	−2.268
45.0, I	0.6611	0.6227	−5.803	0.6636	0.371	0.6460	−2.285
45.0, II	0.5674	0.5369	−5.372	0.5706	0.560	0.5546	−2.251
60.0, I	0.3332	0.3140	−5.752	0.3353	0.630	0.3265	−2.021
60.0, II	0.5022	0.4726	−5.885	0.5055	0.647	0.4913	−2.176
75.0, I	0.0896	0.0859	−4.134	0.0909	1.397	0.0886	−1.127
75.0, II	0.2939	0.2751	−6.390	0.2963	0.828	0.2880	−2.013

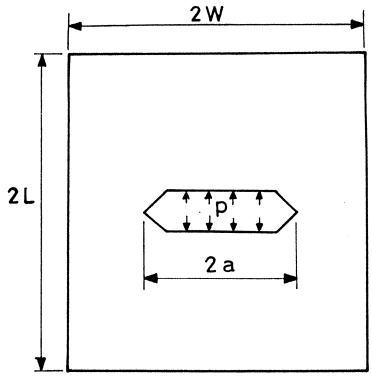

Fig. 4. Centre crack under fluid pressure.

Table 4
Comparison of SIF correction factor Y for centre crack under fluid pressure ($a/w = 0.1$)

	Computed by:								
		Displacement method				CCI method			
		2nd corner node		1st corner node		No external force		With external force	
Reference solution [24]	Element type	Y	% Error	Y	% Error	Y	% Error	Y	% Error
1.0	linear	0.9462	−5.383	0.9002	−9.980	0.9467	−5.330	0.9617	−3.829
1.0	quadratic	0.9765	−2.354	0.9567	−4.328	0.9819	−1.810	1.0085	0.850
1.0	quarter point	0.9907	−0.932	0.9899	−1.006	0.9522	−4.777	0.9825	−1.751

3.5. Kinked crack

This example deals with a single edge kinked crack in a finite plate under uniform tension (Fig. 6). The subregion technique is again employed. Major plate dimensions are: $W = 10$ mm, $L = 30$ mm, $a/W = 0.25\sqrt{2}$. The crack angle θ is 45°. The material properties utilised are: $E = 1$ MPa and $\nu = 0.3$. The loading intensity $\sigma = 10$ MPa. Two $\Delta a/W$ ratios, 0.0125 and 0.025, are examined. The entire plate is subdivided into two regions (Fig. 6b). The total number of elements in each region is restricted to 25 when the quadratic elements are used. The kink is modelled using three elements. There are also three similar elements ahead of the kinked crack tip B. Very similar mesh is used for linear and quarter point elements. In the case of the quarter point elements used around the crack tip, the knee is modelled by ordinary quadratic elements. The computed SIF correction factors Y ($Y = K_{\mathrm{I}}/\sigma\sqrt{(\pi a)}$ or $Y = K_{\mathrm{II}}/\sigma\sqrt{(\pi a)}$) are compared with reference solutions in Table 6.

4. Discussion

Results of the angled edge crack problem are compared with those due to Rooke and Cartwright [28] and Sethuraman [27] (Table 1). The difference in Y is based on the solution of

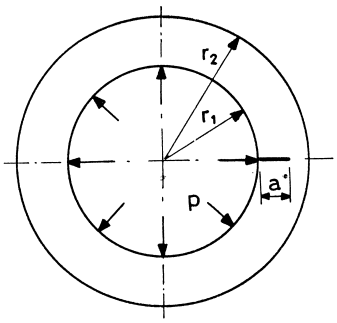

Fig. 5. Radial inner edge crack.

Table 5
Comparison of SIF correction factor Y for cylindrical vessel with radial crack under internal pressure for linear, quadratic and quarter point elements

	SIF correction factor Y								
		Computed by:							
		Displacement method				CCI method			
		2nd corner node		1st corner node		No external force		With external force	
$a/(r_2-r_1)$	Reference solution [30]	Y	% Error	Y	% Error	Y	% Error	Y	% Error
Linear element									
0.2	2.7760	2.5938	−6.563	2.4650	−11.20	2.6162	−5.757	2.6311	−5.218
0.3	2.8672	2.6486	−7.625	2.5174	−12.20	2.6723	−6.796	2.6873	−6.275
0.4	2.9887	2.7419	−8.257	2.6062	−12.80	2.7673	−7.409	2.7822	−6.909
0.5	3.1360	2.8373	−9.525	2.6960	−14.03	2.8624	−8.725	2.8773	−8.248
0.6	3.3152	2.9955	−9.644	2.8458	−14.16	3.0219	−8.846	3.0369	−8.395
0.7	3.5541	3.1968	−10.05	3.0359	−14.58	3.2238	−9.294	3.2387	−8.873
0.8	3.9125	3.5431	−9.442	3.3633	−14.04	3.5716	−8.713	3.5866	−8.330
Quadratic element									
0.2	2.7760	2.6853	−3.266	2.6203	−5.609	2.7412	−1.254	2.7676	−0.303
0.3	2.8672	2.7677	−3.469	2.7012	−5.789	2.8272	−1.397	2.8536	−0.476
0.4	2.9887	2.8898	−3.310	2.8198	−5.651	2.9524	−1.215	2.9788	−0.332
0.5	3.1360	3.0236	−3.584	2.9467	−6.037	3.0845	−1.642	3.1109	−0.801
0.6	3.3152	3.2037	−3.364	3.1189	−5.922	3.2647	−1.522	3.2911	−0.726
0.7	3.5541	3.4276	−3.560	3.3296	−6.318	3.4840	−1.972	3.5104	−1.229
0.8	3.9125	3.7873	−3.201	3.6743	−6.087	3.8440	−1.750	3.8704	−1.075
Quarter point element									
0.2	2.7760	2.7239	−1.877	2.7107	−2.352	2.6547	−4.370	2.6847	−3.289
0.3	2.8672	2.8084	−2.052	2.7954	−2.506	2.7392	−4.466	2.7691	−3.420
0.4	2.9887	2.9329	−1.866	2.9189	−2.337	2.8614	−4.258	2.8914	−3.255
0.5	3.1360	3.0690	−2.138	3.0505	−2.727	2.9898	−4.661	3.0198	−3.705
0.6	3.3152	3.2527	−1.885	3.2297	−2.579	3.1659	−4.504	3.1959	−3.599
0.7	3.5541	3.4810	−2.056	3.4491	−2.955	3.3798	−4.905	3.4098	−4.061
0.8	3.9125	3.8486	−1.633	3.8085	−2.658	3.7316	−4.623	3.7616	−3.856

Ref. [28]. The accuracy of the SIFs is improved through the proposed scheme. The accuracy in the case of the displacement method is always dependent on where the displacements are compared. Generally the SIFs computed by comparing the displacement at the second corner node behind the crack tip are better than those based on the first corner node. The maximum difference is around 10%, 6% and 4.5% for the linear, quadratic and quarter point elements, respectively, when displacement is compared at the first corner node for the entire range of angle θ. This is approximately 8%, 5.5% and 6.5%, respectively, when displacement is compared at the second corner node. This difference reduces to within 6%, 3.2% and 3%, respectively, for the three elements when the proposed MCCI scheme is employed. Further, the results show good agreement with the solutions of Ref. [27], where the FEM is used to

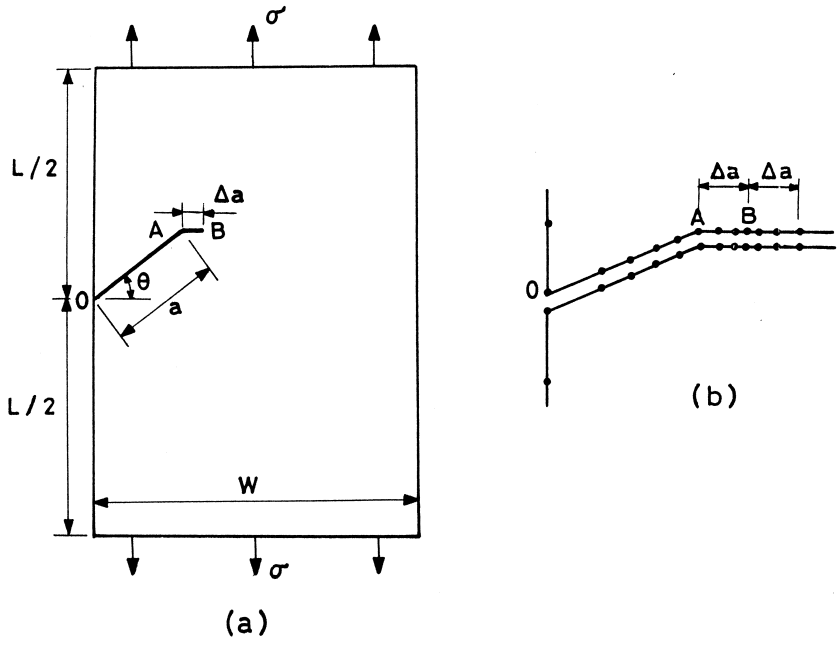

Fig. 6. (a) Edge kinked crack and (b) boundary element mesh over crack span.

compute the SIFs. Notably, in the present analysis the number of nodes employed is 100 as against 524 used by Sethuraman [27].

In the case of the angled crack, the results (Table 2) are compared with the analytical results of Kitagawa et al. [29], which are based on conformal mapping technique with an accuracy better than 0.5%. In this case too the comparison of displacement at the second corner node is preferable to the first corner node. The accuracy is further improved when the MCCI technique is employed. The maximum difference in Y is around 5%, 3.2% and 2%, respectively, when the linear, quadratic and quarter point elements are used for $a/W = 0.2$ and the entire range of θ. A better agreement with the reference solutions is again observed for $a/W = 0.4$ and 0.6 (Table 3).

In the example of centre crack under fluid pressure (Table 4), the computation of SIFs with and without the inclusion of the crack edge loads in the MCCI method provides a measure of the contributions of the external loads on the crack edges. This contribution is around 3% for the quadratic and quarter point elements and about 1.5% for the linear element. This problem has been studied earlier by Maiti [24] using the FEM. The number of degrees of freedom used by him is 942 and the computed SIF has an accuracy of 0.3%. In the present case, the number of degrees of freedom is 96 and the highest accuracy, which is 0.85%, is achieved employing the quadratic elements.

In the example of radial inner edge crack (Table 5), the contributions of external loads acting on the crack edges is less significant than in the earlier case. This effect is about 1% for the quadratic and quarter point elements, and 0.6% for the linear element.

In the example of kinked crack there is a stress singularity at the knee over and above the crack tip stress singularity. The FEM solution of Tracey and Cook [31], which didn't model this knee singularity, differs from the reference solution by 4%. The multipoint singularity

Table 6
Comparison of SIF correction factor Y for single edge kinked crack in a tension strip

		SIF correction factor Y					
					Element types in CCI method		
$\Delta a/w$	Mode	Reference solution [31]	Ref. [32]	Ref. [31] (FEM)	Linear	Quadratic	Quarter point
0.0125	I	42.788	43.184 (0.9%)*	41.076 (–4.0%)	40.316 (–5.78%)	43.664 (2.05%)	41.735 (–2.46%)
0.0125	II	0.000	0.665	0.411	0.041	0.045	0.032
0.0250	I	44.677	44.621 (–0.1%)	43.359 (–4.0%)	42.360 (–5.19%)	45.563 (1.98%)	43.664 (–2.27%)
0.0250	II	0.000	0.130	0.004	0.180	0.111	0.112

* Percentage difference with results of Ref. [31]

elements were employed by Maiti [32] to take care of both the knee and crack tip singularities. In his analysis [32] 754 degrees of freedom were used and the reported results show the maximum difference of 0.9% from the reference solution. In the present study, the knee singularity is not modelled. The number of degrees of freedom is 200. The maximum differences (Table 6) are 2% and 2.5% with the reference solution for the quadratic and quarter point elements, respectively.

5. Conclusions

A boundary element based formulation to evaluate the SIFs under remote and/or crack edge loading through the MCCI technique is proposed. Five case studies have been presented to demonstrate the accuracy of the scheme. The results show that MCCI technique helps in improving the computational accuracy of the SIFs. In the case of fluid pressure type of loading on the crack edges there is an extra contribution to the crack closure work. This must be accounted for a better accuracy of the results. An analysis of the mixed mode problems is as usual facilitated by the subregion technique. However when the crack closure integrals for an in-plane extension are to be evaluated the given domain must be split into subregions carefully. There must be a common interface aligned with the original crack line and extending ahead of the crack tip.

References

[1] Cruse TA. BIE fracture mechanics analysis: 25 years of developments. Computational Mechanics 1996;18:1–11.
[2] Cruse, TA. Numerical evaluation of elastic stress intensity factors by the boundary integral equation method. In *The Surface Crack: Physical Problems and Computational Solutions*, ed. J. L. Swedlow New York: ASME, 1972, pp. 153–170.

[3] Lachat JC, Watson JO. Effective numerical treatment of boundary integral equations: a formulation for three-dimensional elastoplastics. Int. J. Numer. Meth. Engng. 1976;10:991–1005.
[4] Cruse TA. Two-dimensional BIE fracture mechanics analysis. Appl. Math. Modelling 1978;2:287–93.
[5] Tan CL, Fenner RT. Three-dimensional stress analysis by the boundary integral equation method. J. Strain Analysis 1978;13:231–7.
[6] Blandford GE, Ingraffea AR, Liggett JA. Two-dimensional stress intensity factor computations using the boundary element method. Int. J. Numer. Methods Engng. 1981;17:387–404.
[7] van der Weeen F. Mixed mode fracture analysis of rectilinear anisotropic plates using singular boundary elements. Comput. and Struct. 1983;17:469–74.
[8] Martinez J, Dominguez J. On the use of quarter-point boundary elements for stress intensity factor computations. Int. J. Numer. Methods Engng. 1984;20:1941–50.
[9] Karami G, Fenner RT. Analysis of mixed mode fracture and crack closure using the boundary integral equation method. Int. J. Fracture 1986;30:13–29.
[10] Ang WT. A boundary integral solution for the problem of multiple interacting cracks in an elastic material. Int. J. Fracture 1986;31:259–70.
[11] Aliabadi MH, Rooke DP, Cartwright DJ. Mixed-mode Bueckner weight functions using boundary element analysis. Int. J. Fracture 1987;34:131–47.
[12] Aliabadi MH, Rooke DP, Cartwright DJ. An improved boundary element formulation for calculating stress intensity factors: application to aerospace structures. J. Strain Anal. 1987;22:203–7.
[13] Liu SB, Tan CL. Two-dimensional boundary element contact mechanics analysis of angled crack problems. Engng. Fracture Mech. 1992;42:273–88.
[14] Rigby, RH and Aliabadi, MH. 1992. Boundary element analysis of three-dimensional crack problems. In: *Computational Methods in Fracture Mechanics*. eds. MH Aliabadi, H Nisatani and DJ Cartwright. Computational Mechanics Publications, p. 91–105.
[15] Farris TN, Liu M. Boundary element crack closure calculation of three-dimensional stress intensity factors. Int. J. Fracture 1993;60:33–47.
[16] Zeng Z-J, Dai S-H, Yang Y-M. Analysis of surface cracks using line-spring boundary element method and the virtual crack extension technique. Int. J. Fracture 1993;60:157–67.
[17] Guimaraes S, Telles JC F. On the hyper-singular boundary-element formulation for fracture-mechanics applications. Engng. Anal. Boundary Elements 1994;13:353–63.
[18] Selcuk S, Hurd DS, Crouch SL, Gerberich WW. Prediction of interfacial crack path: a direct boundary integral approach and experimental study. Int. J. Fracture 1994;67:1–20.
[19] Gray LJ, Paulino GH. Symmetric Galerkin boundary integral fracture analysis for plane orthotropic elasticity. Comp. Mech. 1997;20:26–33.
[20] Rybicki EF, Kanninen MF. A finite element calculation of stress intensity factors by a modified crack closure integral. Engng. Fracture Mech. 1977;9:931–8.
[21] Krishnamurthy, T, Ramamurthy, TS, Vijayakumar, K and Duttaguru, B. Modified crack closure integral method for higher order finite elements. In: *Proceedings of the International Conference on Finite Elements in Computational Mechanics*.ed. T Kant, 1985, Bombay, p. 891–900.
[22] Sethuraman R, Maiti SK. Finite element based computation of strain energy release rate by modified crack closure integral. Engng. Fracture Mech. 1988;30:227–31.
[23] Maiti SK. Finite element computation of the strain energy release rate for a kinking of a crack. Int. J. Fracture 1990;43:161–74.
[24] Maiti SK. Finite element computation of crack closure integrals and stress intensity factors. Engng. Fracture Mech. 1992;41:339–48.
[25] Maiti SK, Mukhopadhyay NK, Kakodkar A. Boundary element method based computation of stress intensity factors by modified crack closure integral. Computational Mechanics 1997;19:203–10.
[26] Mukhopadhyay NK, Maiti SK, Kakodkar A. Further considerations in modified crack closure integral based computation of stress intensity factor in BEM. Engng. Fract. Mech. 1998;59:269–79.
[27] Sethuraman, R. Analytical and finite element studies on two dimensional panels with doubly bonded rectangular finite crack stiffeners, Ph.D. thesis, Department of Mechanical Engineering, I.I.T. Bombay, India, 1989.
[28] Rooke, DP and Cartwright, DJ. *Compendium of stress intensity factors*. London: HMSO, 1976.

[29] Kitagawa H, Yuuki R. Analysis of arbitrarily shaped crack in a finite plate using conformal mapping, 1-st report—construction of analysis procedure and its applicability. Trans. Japan, Soc. Mech. Engrs. 1977;43:4354–62.
[30] Murakami, Y. *Stress intensity factors handbook*. Oxford: Pergamon Press, 1987.
[31] Tracey DM, Cook TS. Analysis of power type singularities using finite elements. Int. J. Numer. Meth. Engng. 1977;11:1225–33.
[32] Maiti SK. A finite element for variable order singularities based on the displacement formulation. Int. J. Numer. Meth. Engng. 1992;33:1955–74.